HHS Public Access

Author manuscript

Nat Struct Mol Biol. Author manuscript; available in PMC 2012 June 01.

Published in final edited form as:

Nat Struct Mol Biol. ; 18(12): 1424–1427. doi:10.1038/nsmb.2150.

A Shared Structural Solution for Neutralizing Ebolaviruses

João M. Dias[1,7], **Ana I. Kuehne**[2,7], **Dafna M. Abelson**[1], **Shridhar Bale**[1], **Anthony C. Wong**[3], **Peter Halfmann**[4], **Majidat A. Muhammad**[2], **Marnie L. Fusco**[1], **Samantha E. Zak**[2], **Eugene Kang**[2], **Yoshihiro Kawaoka**[4,5], **Kartik Chandran**[3], **John M. Dye**[2], and **Erica Ollmann Saphire**[1,6]

[1]Department of Immunology and Microbial Science, The Scripps Research Institute, La Jolla, CA, USA

[2]Division of Virology, United States Army Medical Research Institute for Infectious Diseases, Fort Detrick, MD USA

[3]Department of Microbiology and Immunology, Albert Einstein College of Medicine, Bronx, NY, USA

[4]Department of Pathobiological Sciences, School of Veterinary Medicine, University of Wisconsin, Madison, WI, USA

[5]Department of Special Pathogens, International Research Center for Infectious Diseases, Institute of Medical Science, University of Tokyo, Tokyo, Japan

[6]The Skaggs Institute for Chemical Biology, The Scripps Research Institute, La Jolla, CA, USA

Abstract

Sudan virus (genus *ebolavirus*) is lethal, yet no monoclonal antibody is known to neutralize it. Here we describe antibody 16F6 that neutralizes Sudan virus and present its structure bound to the trimeric viral glycoprotein. Unexpectedly, the 16F6 epitope overlaps that of KZ52, the only other antibody against the $GP_{1,2}$ core to be visualized. Further, both antibodies against this key GP1–GP2-bridging epitope neutralize at a post-internalization step, likely fusion.

Ebolaviruses (family *Filoviridae*), cause severe hemorrhagic fever with up to 90% fatality. Five antigenically distinct ebolaviruses have been identified that differ in genomic sequence

Correspondence should be addressed to J.M. Dye (john.m.dye1@us.army.mil) and E.O.S. (erica@scripps.edu).

[7]These authors contributed equally to this work.

AUTHOR CONTRIBUTIONS

J.M. Dias determined the crystal structure; S.B. continued refinement; M.L.F. engineered SUDV $GP_{1,2}$ for crystallization; A.K., E.K., S.Z., M.M., and J.M. Dye raised 16F6 and designed and performed BSL-4 neutralization and protection experiments; D.M.A., E.O.S., A.C.W., and K.C. designed and performed cathepsin cleavage and VSIV neutralization experiments; D.M.A., E.O.S., P.H., and Y.K. designed and performed attachment and entry experiments; J.M.Dias, J.M.Dye, D.M.A., S.B., K.C., Y.K., and E.O.S. analyzed results, J.M.Dye, K.C., Y.K., and E.O.S. supervised the research, and J.M.Dias, J.M. Dye, and E.O.S. wrote the manuscript.

COMPETING FINANCIAL INTERESTS

The authors declare no competing financial interests.

ACCESSION CODES

Coordinates and structure factors have been deposited into the PDB under accession code 3S88.

by ~35–45%: Sudan, Ebola, Taï Forest, Reston, and Bundibugyo. However, almost all human deaths result from infection with either Sudan virus (SUDV; formerly known as Sudan ebolavirus) or Ebola virus (EBOV; formerly known as Zaire ebolavirus). In October 2000, a new variant of SUDV, termed Gulu (SUDV-Gul)[1], emerged in the Gulu district of northwestern Uganda. It triggered the largest outbreak of Ebola hemorrhagic fever yet described, involving at least 425 individuals, of whom 224 died[2]. Multiple monoclonal antibodies against EBOV have been developed[3–7], but very few of them are known to neutralize and none of them neutralizes SUDV. Development and characterization of SUDV-specific monoclonal antibodies is essential for provision of diagnostic reagents, immunotherapeutics and vaccines. Hence, we set out to raise monoclonal antibodies against SUDV and to structurally map their epitopes on the viral glycoprotein.

The entry of ebolaviruses is a multi-step process including attachment to target cells, internalization into endosomes, and fusion with endosomal membranes. The ebolavirus surface glycoprotein $GP_{1,2}$ is the sole virus protein responsible for these processes. $GP_{1,2}$ is expressed as a 676 amino-acid precursor that is post-translationally cleaved by furin to yield two subunits, GP1 and GP2 (ref. 8). GP1 and GP2 remain covalently linked by a disulfide bond[9], and the resulting GP1-GP2 pair trimerizes to form a ~450 kDa envelope spike on the viral surface. GP1 is responsible for attachment to new host cells, while GP2 mediates fusion of the virus envelope with cellular endosomal membranes. GP1 contains base, head, glycan cap, and mucin-like domains. The head subdomain contains putative receptor-binding regions and is capped by the heavily glycosylated “glycan cap” and mucin-like domain. In the endosome, a flexible loop containing GP1 residues 190–213 is cleaved by host cathepsins[10,11]. This cleavage releases the glycan cap and mucin-like domains from GP1. Also in the endosome, GP2 releases from GP1 and undergoes irreversible conformational changes that drive fusion with host endosomal membranes. GP2 contains an N-terminal peptide, a hairpin-forming fusion loop, and two heptad repeats connected by a functionally important linker. The first heptad repeat of GP2 is wound around the base of GP1 in a metastable, prefusion-specific conformation (Supplementary Fig. 1).

To generate antibodies specific for SUDV, BALB/c laboratory mice were vaccinated with Venezuelan equine encephalitis virus (VEEV) replicons bearing SUDV (strain Boniface) $GP_{1,2}$, and boosted with γ-radiation-inactivated SUDV-Boniface. Among the resulting monoclonal antibodies, IgG_1 16F6 was found to be directed against a conformational epitope on $GP_{1,2}$, to be specific for SUDV, and to react with at least two different SUDV variants, Boniface and Gulu. A trimeric complex of SUDV-Gulu $GP_{1,2}$ in complex with 16F6 Fab fragment was crystallized to map the epitope of 16F6 and understand its SUDV specificity.

SUDV-Gulu $GP_{1,2}$ was expressed for crystallization by transient transfection of human embryonic kidney 293T cells. No mutations of the N-linked glycosylation sites were required, as were necessary for crystallization of EBOV $GP_{1,2}$ (refs. 12,13). SUDV-Gulu $GP_{1,2}$-16F6 crystallizes in the space group I23 with one monomeric $GP_{1,2}$ -Fab complex in the asymmetric unit (Supplementary Table 1). The biologically relevant trimer is formed by crystallographic symmetry, and $GP_{1,2}$ is in its supposed metastable, prefusion conformation (Figure 1).

In general, the SUDV $GP_{1,2}$ crystals are better ordered than those of EBOV $GP_{1,2}$, allowing visualization of outer portions of the glycan cap and the linker region between the N- and C-terminal heptad repeats of GP2, neither of which were previously observed (Figure 1c). The linker region contains a CX_6CC motif, in which the first two cysteines, Cys 601 and Cys 608, form an intra-GP2 disulfide bond that anchors the intervening polypeptide in a cloverleaf loop (Figure 1d). The third Cys (Cys 609) anchors the GP2 cloverleaf to Cys 53 in the base of GP1 (Figure 1d). The shape and location of these disulfide-anchored loops suggest that they restrict flexibility between N-terminal and C-terminal heptad repeats to an elbow-like range of motion, perhaps coupling the rotation of GP1 with the second heptad repeat of GP2 during membrane fusion.

The N-terminal half of the GP2 fusion loop is only 33% conserved between the two viruses and adopts a different, lower-hanging conformation (Figure 1c). By contrast, the C-terminal half of the fusion loop is conserved in sequence and structure between SUDV and EBOV, and is anchored to the outside of the trimer by Arg 89 of the neighboring monomer's GP1 head subdomain (Supplementary Fig. 2). In SUDV, Arg 89 forms five hydrogen bonds and a hydrophobic contact to the fusion loop. These contacts are conserved between SUDV and EBOV structures, and Arg 89 is likely critical for clamping the fusion loop in place to anchor the trimer in its prefusion conformation (Supplementary Fig. 2a).

In the proposed three-dimensional receptor-binding site of GP1 (head subdomain), regions that project are conserved in sequence, while regions that are recessed differ in sequence between SUDV and EBOV (Figure 2a and Supplementary Figs. 3–4). The conserved, projecting regions (residues 114–120, 144–147, 149, and 172–173) may thus delineate surfaces expected to bind to the shared receptor.

More of the cathepsin-cleavage site polypeptide is visible in the SUDV structure than in the EBOV structure. The position of the newly observed residues (190–192 and 212–213) immediately above and below the fusion loop suggests that the GP2 fusion loop could be tethered by the 190–213 polypeptide (Supplementary Fig. 2b). Regions of $GP_{1,2}$ that surround the cathepsin cleavage site and that line the trimer interface differ in sequence between SUDV and EBOV. Unexpectedly, these sequence variations cause distinctly different electrostatic charges in the $GP_{1,2}$ peplomers. SUDV $GP_{1,2}$ is acidic overall, especially at the base of the trimer where the metastable $GP_{1,2}$ assembly intertwines. By contrast, EBOV $GP_{1,2}$ is more neutral, and slightly basic where GP1 and GP2 intertwine (Figure 2b–c, Supplementary Fig. 3).

The crystal structure reveals that mAb 16F6 binds to the base of the SUDV $GP_{1,2}$ trimer and directly bridges the base of GP1 to the stem of the internal fusion loop of GP2 (Figure 1, Supplementary Fig. 2c). Unexpectedly, the epitope of 16F6 overlaps that of mAb KZ52, the only other antibody against the core of any ebolavirus $GP_{1,2}$ to be structurally mapped[13] (Figure 3). KZ52 is specific for EBOV $GP_{1,2}$ and was identified in a library derived from a human survivor of the Kikwit, Zaire outbreak in 1995 (ref. 3). The 16F6 and KZ52 epitopes have a central nine residues in common: 42–44 of GP1 and 513, 550–553 and 556 of GP2 (Figure 3b). Six of these nine are conserved between SUDV and EBOV (Supplementary Fig. 4). Fundamentally, although the two antibodies were produced against distinct viruses and in

different immunological contexts (one by a vaccinated mouse, the other by a naturally infected human), these antibodies recognize overlapping epitopes and have arrived at a shared, structural solution for neutralizing ebolaviruses.

16F6 recognizes native $GP_{1,2}$ on the surface of cells infected with Sudan virus (Supplementary Fig. 5a). Plaque reduction neutralization tests (PRNT) illustrate that 16F6 confers a >99% reduction of SUDV plaques (100 pfu) at 20 μg ml^{-1} (Supplementary Fig. 5b). Plaque reduction occurs in the presence or absence of complement, indicating that binding of 16F6 alone is sufficient to block SUDV infection *in vitro*. Furthermore, intraperitoneal treatment of SCID mice with 100 μg of 16F6 every 5 days after SUDV infection delayed the death of mice by ~ 4 days ($p<0.0001$; Supplementary Fig. 5c).

By pseudotyping SUDV or EBOV $GP_{1,2}$ onto vesicular stomatitis Indiana virus (VSIV), we can achieve a direct comparison of the ability of 16F6 and KZ52 to neutralize otherwise identical virions bearing their cognate surface antigens. Neutralization activity of 16F6 is a bit better than that of KZ52: >99% vs. ~90% reduction of 293T cell transduction at equal concentrations (Supplementary Fig. 5d). Improvements in neutralization capacity are critical for provision of immunotherapeutics against ebolaviruses, for which doses of a single pfu can be lethal.

Separate attachment and internalization assays indicate that $GP_{1,2}$-pseudotyped VSIV attach to and enter Vero E6 cells even in presence of saturating quantities of 16F6 or KZ52 (Supplementary Fig. 6a), and that KZ52 neutralizes VP30-deleted, biologically contained EBOV[14] at a post-entry step (Supplementary Fig. 6b; a biologically contained Sudan virus is not yet available). Consequently, antibodies against the shared 16F6 and KZ52 site must neutralize at a post-attachment, post-internalization step. Another step in the ebolavirus life cycle is cleavage of GP1 by cathepsins in the endosome[15,16]. However, neither 16F6 nor KZ52 inhibit cathepsin L cleavage of either recombinant or viral surface GP1. Even in the presence of a tenfold molar excess of KZ52 and 16F6, SUDV and EBOV $GP_{1,2}$ are fully digested by cathepsin L within 30 min and 60 min, respectively (Supplementary Fig. 7).

Because 16F6 and KZ52 function after internalization and do not inhibit cathepsin L cleavage, two possible mechanisms of inhibition remain: 16F6 and KZ52 may inhibit the function of some other unidentified factor, such as a co-receptor. Alternately, 16F6 and KZ52 may prevent conformational changes in $GP_{1,2}$ required for membrane fusion. Structural evidence supports the latter: both 16F6 and KZ52 physically link GP1 to GP2 and are specific for their prefusion conformation. Furthermore, the conformational changes in GP2 required for membrane fusion could not occur while 16F6 or KZ52 remain bound. Indeed, the greater neutralization capacity of 16F6 may be related to its more effective linkage of GP1 to GP2. The $GP_{1,2}$ surface buried by 16F6 binding is composed of 60% GP1 and 40% GP2. By contrast, the $GP_{1,2}$ surface buried by KZ52 is composed of 20% GP1 and 80% GP2. Importantly, these antibodies are likely to remain bound to $GP_{1,2}$ in the endosome: crystals of the EBOV $GP_{1,2}$-KZ52 complex generated at pH 4.8 exhibit unit cell dimensions identical to those developed at neutral or basic pH[12], and $GP_{1,2}$ pre-treated at pH 5.0 is well-recognized by KZ52 (ref. 13). Hence, pH alone is insufficient to separate GP1 from GP2.

This better-ordered $GP_{1,2}$ structure allowed us to predict conformational rearrangements that may occur during membrane fusion of all ebolaviruses. Arg 89 is proximal to the proposed receptor-binding site in the GP1 head. Its hold on the neighboring monomer's fusion loop must be released for fusion to occur, an action that could be accomplished directly by receptor binding, indirectly by conformational change transmitted by neighboring residues that do bind receptor, or by continued enzymatic processing of GP1. Subsequent unwinding of the fusion loops from the outside of the trimer could be facilitated by cathepsin cleavage of the 190–213 loop, which may loosely tether GP2 in place (Supplementary Fig. 2b). Motion of the fusion loops may be coupled to unwinding of the C-terminally linked heptad repeat 1 (HR1) from its GP1 spool into its single, extended postfusion helix[17,18] and to the subsequent rotation of HR2 towards the target cell to form a six-helix bundle (Supplementary Fig. 1).

Antibodies against the fusion subunits of influenza A virus hemagglutinin (HA) are known to block viral fusion[19,20]. Interestingly, the anti-HA antibodies recognize only the fusion subunit, while 16F6 and KZ52 bind both the fusion subunit and the receptor-binding subunits of the glycoprotein and physically anchor them together. Hence, the shared epitope of 16F6 and KZ52 suggests a unique structural strategy by which antibodies inhibit viral infection.

In summary, we have demonstrated efficacy *in vitro* and *in vivo* of the first antibody shown to neutralize Sudan virus, and have crystallized it in complex with the oligomeric, prefusion SUDV (Gulu) $GP_{1,2}$. This structure and accompanying mechanistic analysis reveal new insights into ebolavirus entry and demonstrate that antibodies elicited in two unique host species by different scenarios bind overlapping epitopes and function at a similar post-entry step. Their overlapping epitopes may indicate a key site for neutralization of ebolaviruses. Further, this work suggests that for viruses in general, antibodies that anchor glycoprotein subunits together and prevent conformational changes required for fusion may be key targets for immunotherapy and key goals of vaccine design.

Supplementary Material

Refer to Web version on PubMed Central for supplementary material.

Acknowledgments

We thank Drs. Dennis Burton and Ann Hessell of The Scripps Research Institute (TSRI) for KZ52, Dr. Michael Whitt of the University of Tennessee Health Science Center and Dr. Douglas Lyles of Wake Forest University School of Medicine for anti-VSV IgG 23H12, Dr. James Cunningham of Brigham and Women's Hospital for rabbit anti-GP1 polyclonal antibody and Dr. Ian Wilson of TSRI for critical reading of the manuscript. We would also like to thank the staff of the Advanced Photon Source Beamline 19-ID and the Advanced Light Source Beamlines 8.2.2 and 8.3.1 for assistance and use of their DOE-supported facilities. E.O.S. wishes to acknowledge NIH grant U01 AI070530, the Skaggs Institute for Chemical Biology, a Career Award in the Biomedical Sciences and an Investigator in the Pathogenesis of Infectious Disease Award from the Burroughs Welcome Fund. K.C. acknowledges support from NIH grants K22 AI074908 and R21 AI082437 and institutional funds of the Albert Einstein College of Medicine. Y.K. acknowledges support from NIH R01 AI055519 and membership within and support from the Region V 'Great Lakes' Regional Center for Excellence for Biodefense and Emerging Infectious Diseases Research (RCE) Program (NIH award 2 U54 AI057153). J.M. Dye wishes to acknowledge support from DTRA K.K0001_07_RD_B. Opinions, interpretations, conclusions and recommendations are those of the authors and are not necessarily endorsed by the U.S. Army. Research was conducted in compliance with the Animal Welfare Act, other federal statutes and regulations relating to animals and experiments involving animals,

principles stated in the Guide for the Care and Use of Laboratory Animals (National Research Council, 1996). The animal facility where this research was conducted is fully accredited by the Association for the Assessment and Accreditation of Laboratory Animal Care International.

References

1. Sanchez A, Rollin PE. Virus Res. 2005; 113:16–25. [PubMed: 16139097]
2. Okware SI, et al. Trop Med Int Health. 2002; 7:1068–75. [PubMed: 12460399]
3. Maruyama T, et al. J Infect Dis. 1999; 179(Suppl 1):S235–9. [PubMed: 9988189]
4. Takada A, et al. J Virol. 2003; 77:1069–74. [PubMed: 12502822]
5. Wilson JA, et al. Science. 2000; 287:1664–6. [PubMed: 10698744]
6. Shahhosseini S, et al. J Virol Methods. 2007; 143:29–37. [PubMed: 17368819]
7. Yu JS, et al. J Virol Methods. 2006; 137:219–28. [PubMed: 16857271]
8. Volchkov VE, Feldmann H, Volchkova VA, Klenk HD. Proc Natl Acad Sci U S A. 1998; 95:5762–7. [PubMed: 9576958]
9. Jeffers SA, Sanders DA, Sanchez A. J Virol. 2002; 76:12463–72. [PubMed: 12438572]
10. Dube D, et al. Journal of Virology. 2009; 83:2883–2891. [PubMed: 19144707]
11. Hood CL, et al. Journal of Virology. 2010; 84:2972–82. [PubMed: 20053739]
12. Lee JE, Fusco ML, Hessell AH, Burton DR, Saphire EO. Acta Crystallographica. 2009; D65:1162–1180. [PubMed: 19923712]
13. Lee JE, et al. Nature. 2008; 474:177–183. [PubMed: 18615077]
14. Halfmann P, et al. Proc Natl Acad Sci U S A. 2008; 105:1129–33. [PubMed: 18212124]
15. Chandran K, Sullivan NJ, Felbor U, Whelan SP, Cunningham JM. Science. 2005
16. Schornberg K, et al. J Virol. 2006; 80:4174–8. [PubMed: 16571833]
17. Weissenhorn W, Carfi A, Lee KH, Skehel JJ, Wiley DC. Mol Cell. 1998; 2:605–16. [PubMed: 9844633]
18. Malashkevich VN, et al. Proc Natl Acad Sci U S A. 1999; 96:2662–7. [PubMed: 10077567]
19. Ekiert DC, et al. Science. 2009; 324:246–51. [PubMed: 19251591]
20. Sui J, et al. Nat Struct Mol Biol. 2009; 16:265–73. [PubMed: 19234466]

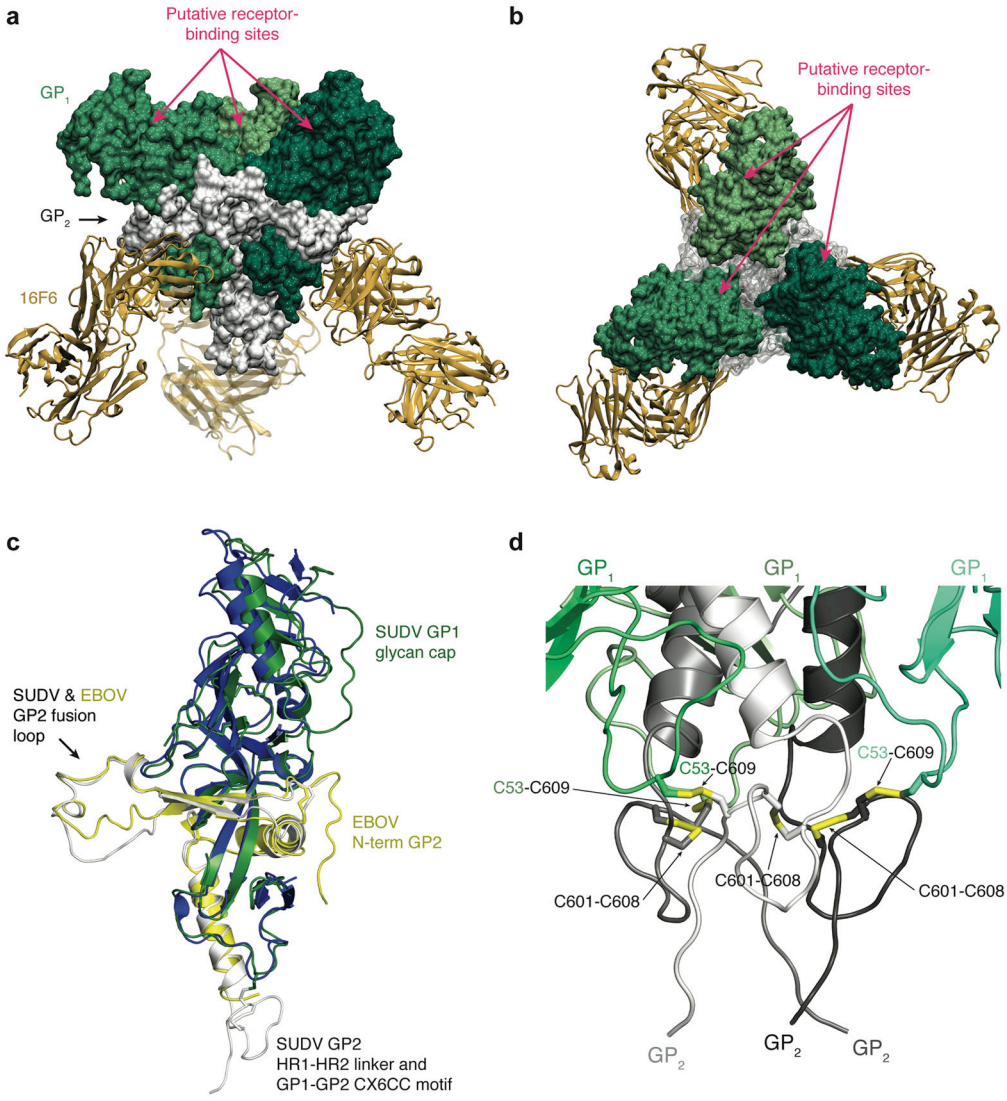

Figure 1.

Structure of Sudan virus (SUDV) $GP_{1,2}$ in complex with Fab 16F6. GP1 subunits are colored three different shades of green, GP2 subunits are white, and bound 16F6 Fab fragments are gold. (**a**) Side view with viral membrane toward bottom and target cell toward the top. Note that 16F6 binds the base of the $GP_{1,2}$ peplomer, distal from putative receptor-binding sites. (**b**) Top view, from the perspective of the target cell. Putative receptor-binding sites are indicated by pink circles. (**c**) Superposition of the SUDV and Ebola virus (EBOV) $GP_{1,2}$ monomers. SUDV GP1–GP2 is colored green for GP1 and white for GP2, while EBOV GP1–GP2 is colored blue for GP1 and yellow for GP2. The SUDV structure includes additional regions of the glycan cap (top), the linker between heptad repeats 1 and 2 (HR1 and HR2) and the CX6CC motif (bottom), although the N terminus of GP2 is disordered. (**d**) The linker region between HR1 and HR2 forms two disulfide bonds per monomer: one linking GP1 to GP2 (Cys 53-Cys 609) and one within GP2 (Cys 601-Cys 608). All Figures have been generated with PyMOL and VMD.

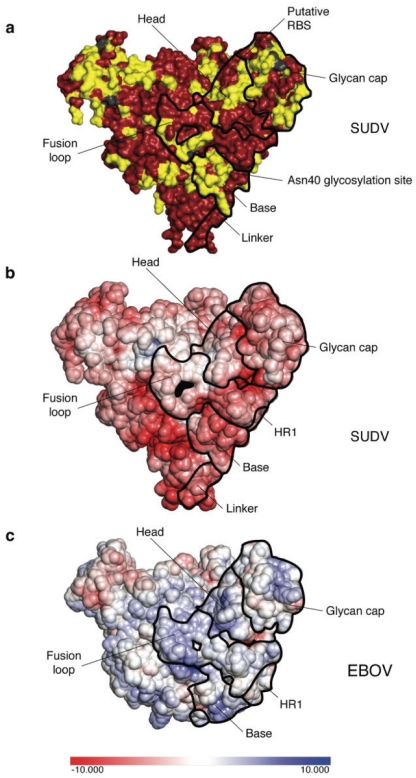

Figure 2.

Surfaces of SUDV GP. (**a**) Sequence conservation. Residues that are identical between SUDV and EBOV are colored red, while these that are different are colored yellow. The domains of one $GP_{1,2}$ monomer are outlined in black with subdomains indicated. (**b**) Electrostatic potential representation of the SUDV $GP_{1,2}$ surface with limits +/− 10 keT. (**c**) Electrostatic potential representation of the EBOV $GP_{1,2}$ surface with limits +/− 10 keT.

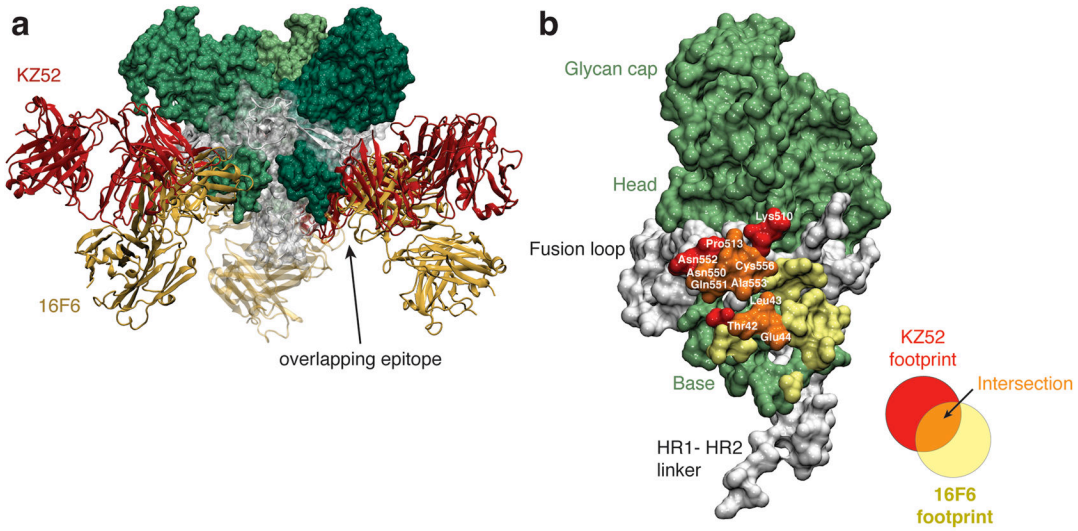

Figure 3.

16F6 epitope. (**a**) mAbs 16F6 and KZ52 recognize similar GP1–GP2-bridging epitopes (black oval). Here, the structure of SUDV $GP_{1,2}$ in complex with 16F6 (gold) is superimposed with the structure of EBOV $GP_{1,2}$ in complex with KZ52 (brick red). Only the SUDV $GP_{1,2}$ trimer (green and white) is shown for clarity. (**b**) Epitope footprints of 16F6 (yellow) and KZ52 (red) are mapped onto the SUDV surface, for which a single $GP_{1,2}$ monomer is shown in green for GP1 and white for GP2. Residues shared between the two antibody epitopes (T42, L43, E44, P513, N550, Q551, N552, A553 and C556) are colored orange.